

Long non-coding RNA IRAIN suppresses apoptosis and promotes proliferation by binding to LSD1 and EZH2 in pancreatic cancer

Yifan Lian¹ · Juan Wang¹ · Jing Feng² · Jie Ding¹ · Zhonghua Ma¹ · Juan Li¹ · Peng Peng³ · Wei De⁴ · Keming Wang¹

Received: 11 April 2016 / Accepted: 9 September 2016 / Published online: 19 September 2016
© International Society of Oncology and BioMarkers (ISOBM) 2016

Abstract Long non-coding RNA (lncRNA) modulates gene expression, while lncRNA dysregulation is associated with human cancer. Furthermore, while recent studies have shown that lncRNA IRAIN plays an important role in other malignancies, the role of IRAIN in pancreatic cancer (PC) progression remains unclear. In this study, we found that upregulation of lncRNA IRAIN was significantly correlated with tumor size, TNM stage, and lymph node metastasis in a cohort of 37 PC patients. In vitro experiments showed that knockdown of IRAIN by small interfering RNA (siRNA) significantly induced cell apoptosis and inhibited cell proliferation in both BxPC-3 and PANC-1 cells. Further mechanism study showed that, by binding to histone demethylase lysine-specific demethylase 1 (LSD1), an enhancer of zeste homolog 2 (EZH2), IRAIN reduced PC tumor cell apoptosis and induced growth arrest by silencing the expression of Kruppel-like factor 2 (KLF2) and P15. Moreover, IRAIN expression was inversely correlated with that of KLF2 and P15 in PC tissues. To

our knowledge, this is the first report elucidating the role and mechanism of IRAIN in PC progression.

Keywords Pancreatic cancer · Apoptosis · lncRNA · IRAIN · LSD1 · EZH2

Introduction

Pancreatic cancer is one of the most aggressive malignancies and the fourth most common cause of cancer death in the USA, with an estimated 40,560 deaths in 2015 [1]. In contrast to the steady increase in survival for most cancers, advances have been slow for pancreatic cancer, for which the 5-year relative survival is currently only 7 % [1]. Reasons for the dismal prognosis include complex pancreatic tumor biology, early metastasis, late diagnosis, and limited efficiency of current therapies [2, 3]. Hence, understanding the molecular mechanisms of tumor progression could have a significant impact on early pancreatic cancer detection and intervention.

The development of high-throughput DNA sequencing and array-based technologies has facilitated the identification of numerous new long non-coding RNAs (lncRNAs). Briefly, lncRNAs are a type of RNA molecule larger than 200 nucleotides that do not encode proteins [4]. Because they lack open reading frames, they were originally considered to be transcriptional noise [5]. However, mounting evidence suggests that lncRNAs have key roles in gene regulation and thus affect various aspects of tumor cellular homeostasis, including proliferation, differentiation, apoptosis, and metastasis [6]. For example, our previous study demonstrated that the lncRNA HOXA transcript at the distal tip (HOTTIP) promotes colorectal cancer growth and inhibits cell apoptosis, partially via downregulation of p21 expression [7]. However, the contributions of aberrant lncRNAs to pancreatic cancer development

Yifan Lian, Juan Wang, and Jing Feng contributed equally to the work.

✉ Keming Wang
kemingwang@njmu.edu.cn

- ¹ Department of Oncology, Second Affiliated Hospital, Nanjing Medical University, Nanjing 210000, Jiangsu, People's Republic of China
- ² Department of Oncology, First Affiliated Hospital of Nanjing Medical University, Nanjing 210000, Jiangsu, People's Republic of China
- ³ Department of Oncology, The Second Hospital of Nanjing, Nanjing 210000, Jiangsu, People's Republic of China
- ⁴ Department of Biochemistry and Molecular Biology, Nanjing Medical University, Nanjing 210000, Jiangsu, People's Republic of China

and progression and their underlying molecular mechanisms are not well documented.

Recently, studies have indicated that numerous lncRNAs contribute to cancer cell phenotypes through the silencing of tumor suppressors or activation of oncogenes via interaction with specific RNA-binding proteins (RBPs) [8–12]. For example, lncRNA PVT1 promotes thyroid cancer cell proliferation by recruiting EZH2 and regulating thyroid-stimulating hormone receptor expression [13]. Dysregulation of the lncRNA LINC01133 suppresses Kruppel-like factor 2 (KLF2), P21, and E-cadherin transcription by interacting with EZH2 and lysine-specific demethylase 1 (LSD1) in non-small cell lung cancer [14]. Therefore, other lncRNAs may also contain multiple binding sites for distinct protein complexes that directly modulate target gene expression.

lncRNA IRAIN, which is 5359 nt in length, is located in chromosome 15q26.3. Current studies have found that lncRNA IRAIN may contribute to the progression of non-small cell lung cancer (NSCLC) and that its expression level is significantly upregulated in NSCLC tissues and connected with tumor size and smoking status [15]. However, the functional role and underlying mechanism of IRAIN in pancreatic cancer (PC) remain to be clarified. In this study, we investigated IRAIN expression in pancreatic cancer, assessed its biological functions, and performed an initial analysis of its molecular mechanisms of action.

Materials and methods

Tissue samples

A total of 37 paired PC and adjacent non-tumor pancreas tissues were obtained from patients with PC who had undergone surgery at the Second Affiliated Hospital, Nanjing Medical University, from 2014 to 2016. All cases were confirmed as PC based on histopathological evaluation. No prior treatment had been conducted before surgery. Clinicopathological characteristics were recorded in detail. All collected tissue samples were rapidly snap frozen in liquid nitrogen and stored at -80°C until RNA extraction. Informed consent was obtained from all patients. Our study was approved by the Research Ethics Committee of Nanjing Medical University, China.

RNA extraction and qPCR assays

Total RNA was extracted from tissues or cultured cells using TRIzol reagent (Invitrogen, Carlsbad, CA) according to the manufacturer's protocol. RNA quantity and quality were determined by NanoDrop 2000c (Thermo Scientific, Waltham, MA, USA). For qRT-PCR, 1 μg of RNA was reverse transcribed to cDNA using a Reverse Transcription Kit (Takara,

Dalian, China). The qPCR assays were conducted on an ABI 7500. Data were normalized to the expression of glyceraldehyde-3-phosphate dehydrogenase (GAPDH). Primers used for target amplification are listed in Table 1. All qPCR data were calculated and expressed relative to the threshold cycle (shown as ΔCT) values and then converted to fold changes.

Cell lines and culture conditions

Three PC cell lines (AsPC-1, BxPC-3, and PANC-1) and HPDE6 cells (immortalized human pancreatic ductal epithelial cells) were purchased from the Institute of Biochemistry and Cell Biology of the Chinese Academy of Sciences (Shanghai, China). The cells were cultured in RPMI 1640 or DMEM (GIBCO-BRL) medium supplemented with 10 % fetal bovine serum (10 % FBS), 100 U/ml penicillin, and 100 mg/ml streptomycin in humidified air at 37°C with 5 % CO_2 .

Cell transfection

PC cells were transfected with small interfering RNA (siRNA) oligonucleotides with plasmids using Lipofectamine 2000 (Invitrogen, USA) according to the manufacturer's protocol. The siRNAs were purchased from Invitrogen (Invitrogen, USA). The nucleotide sequences of siRNA for the experiment are also listed in Table 1. After 48 h of transfection, the cells were harvested for further study.

Table 1 Sequences of primers for qPCR and siRNA sequence

Name	Sequences (5' to 3')
Primers for qPCR	
IRAIN (forward)	CGACACATGGTCCAATCACTGTT
IRAIN (reverse)	AGACTCCCCTAGGACTGCCATCT
GAPDH (forward)	GAAGAGAGAGACCCTCACGCTG
GAPDH (reverse)	ACTGTGAGGAGGGGAGATTCACT
KLF2 (forward)	CTGCACATGAAACGGCACAT
KLF2 (reverse)	CAGTCACAGTTTGGGAGGGG
P15 (forward)	GGACTAGTGGAGAAGGTGCG
P15 (reverse)	GGGCGCTGCCATCATCATG
LSD1 (forward)	AGCGTCATGGTCTTATCAA
LSD1 (reverse)	GAAATGTGGCAACTCGTC
EZH2 (forward)	TGCACATCCTGACTTCTGTG
EZH2 (reverse)	AAGGGCATTACCAACTCC
Interference sequences (siRNA)	
si-IRAIN	GGCAACCAUUACUCACCAATT
si-NC	UUCUCCGAACGUGUCACGUTT
si-LSD1	GCCACCCAGAGAUUUACUTT
si-EZH2	GAGGUUCAGACGAGCUGAUUU

Cell viability and colony formation assay

Cell viability was monitored using a Cell Proliferation Reagent Kit I (MTT; Roche Applied Science). The BxPC-3 and PANC-1 cells were transfected with si-IRAIN or si-NC (3000 cells/well) and were cultured in 96-well plates with six replicate wells. Cell viability was assessed according to the manufacturer's recommendations. For the colony formation assay, a total of 500 cells were placed in a six-well plate and maintained in medium containing 10 % FBS, which was replaced every 5 days. After 2 weeks, cells were fixed with methanol and stained with 0.1 % crystal violet (Sigma-Aldrich). Visible colonies were manually counted. Triplicate wells were measured in each treatment group.

Flow cytometry

BxPC-3 and PANC-1 cells transfected with si-IRAIN or si-NC were harvested after 48 h for apoptosis analysis. The cells were then treated with fluorescein isothiocyanate (FITC)-annexin V and propidium iodide (PI) in the dark at room temperature according to the manufacturer's recommendations. Subsequently, the cells were analyzed by FACScan[®] and identified as viable, dead, early apoptotic, or late apoptotic cells.

BxPC-3 and PANC-1 cells transfected with si-IRAIN or si-NC were harvested after 48 h. They were then stained with PI using a Cycletest[™] Plus DNA Reagent Kit (BD Biosciences) according to the manufacturer's protocol and analyzed with a flow cytometer (FACScan[®]; BD Biosciences) equipped with CellQuest software (BD Biosciences). The percentages of the cells in G0/G1, S, and G2/M phases were calculated and compared.

TUNEL assay

Apoptotic cells were detected using the terminal deoxynucleotidyl transferase dUTP nick end labeling (TUNEL) assay (In Situ Cell Death Detection Kit, Roche). In brief, BxPC-3 and PANC-1 cells were incubated in proteinase K for 15 min at room temperature. After rinsing twice in phosphate-buffered saline (PBS) for 2 min each time, the sections were incubated in 0.1 % Triton X-100 in 1 % sodium citrate on ice for 2 min. They were then labeled (60 min, 37 °C) with a fluorescein-TUNEL reagent mixture according to the manufacturer's instructions. After rinsing three times with PBS, apoptotic cells were photographed by fluorescence microscopy (OLYMPUS IX71; Olympus Corporation, Tokyo, Japan), and representative images were captured using a camera. The nuclei were stained using 4',6-diamidino-2-phenylindole (DAPI).

Western blot assay and antibodies

BxPC-3 and PANC-1 cells were lysed with RIPA protein extraction reagent (Beyotime, Beijing, China) supplemented with a protease inhibitor cocktail (Roche, CA, USA). Protein extracts (40 µg) were separated by 10 % SDS-polyacrylamide gel electrophoresis (SDS-PAGE) and then transferred to 0.22-µm nitrocellulose membranes (Sigma) and incubated with anti-P21 antibody, anti-cleaved caspase-3 antibody, anti-Bcl-2 antibody, anti-P15 antibody, or anti-KLF2 antibody. GAPDH antibody was used as a control. Both antibodies were purchased from Sigma-Aldrich (USA). ECL chromogenic substrate was used, and signals were quantified by densitometry (Quantity One software, Bio-Rad).

RIP assay

RNA immunoprecipitation (RIP) experiments were performed using a Magna RIP RBP Immunoprecipitation Kit (Millipore) according to the manufacturer's instructions. Antibodies for RIP assays against EZH2 and LSD1 were purchased from Millipore. Briefly, BxPC-3 cells at 80–90 % confluency were scraped off and then lysed in complete RIP lysis buffer, after which 100 µl of whole cell extract was incubated with RIP buffer containing magnetic beads conjugated with human anti-EZH2 antibody (Millipore), anti-LSD1 antibody (Millipore), and negative control normal mouse IgG (Millipore). Samples were incubated with proteinase K with shaking to digest the protein, and then, immunoprecipitated RNA was isolated. RNA concentration was measured using a NanoDrop spectrophotometer (Thermo Scientific), while RNA quality was assessed using a bioanalyzer (Agilent, Santa Clara, CA, USA). The RNA from the IP materials was further assessed by qPCR analysis.

Statistical analysis

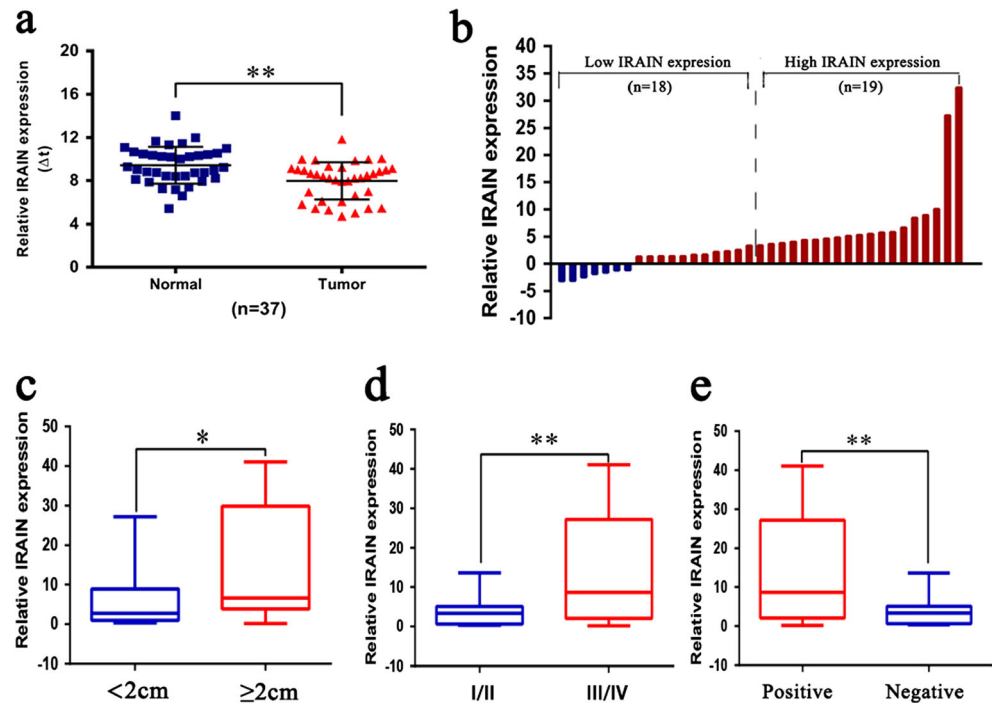
All statistical analyses were performed using SPSS software, version 22.0 (SPSS, Chicago, IL, USA). Student's *t* test or a chi-square test was used to evaluate significant differences between groups of data. All data are represented as means ± SD. Differences were considered significant if $P < 0.05$. “*” indicates $P < 0.05$; “***” indicates $P < 0.01$.

Results

IRAIN expression was upregulated and correlated with advanced pathological stage, larger tumor size, and lymph node metastasis in patients with PC

IRAIN expression levels were detected in 37 paired PC samples. Adjacent normal tissues were analyzed with qPCR and

Fig. 1 Increased IRAIN expression in PC tissues and its clinical significance. **a, b** Relative expression of IRAIN in PC tissues compared with corresponding adjacent normal tissues ($n = 37$). **c–e** Results are presented as the relative expression level in tumor tissues. IRAIN expression was significantly higher in patients with a larger tumor size, a higher pathological stage, and lymph node metastasis (shown as ΔCT). Bars: SD, * $P < 0.05$, ** $P < 0.01$, from three independent experiments



normalized to GAPDH. The results showed that IRAIN expression levels were remarkably higher in the tumor tissues than in the adjacent normal tissues ($P < 0.01$; Fig. 1a). Next, in order to investigate the relationship between IRAIN expression and clinical pathological features, we divided the samples into high (above the median, $n = 19$) and low (below the median, $n = 18$) IRAIN expression groups according to the median value of IRAIN levels (Fig. 1b). A chi-square test was then performed to evaluate the clinicopathological features between the two groups. As shown in Fig. 1c–e, increased IRAIN expression levels in PC were significantly correlated with larger tumor sizes ($P = 0.049$), advanced TNM stages ($P = 0.020$), and lymph node metastasis ($P = 0.020$). However, several other clinical parameters were found not to be significantly associated with IRAIN expression (Table 2).

Modulation of IRAIN expression in PC cells

We next performed qPCR analysis to examine the expression of IRAIN in three human PC cell lines, including AsPC-1, BxPC-3, and PANC-1, and immortalized human pancreatic ductal epithelial cells (HPDE6 cells). We found that IRAIN expression was significantly upregulated in AsPC-1 ($P < 0.01$), BxPC-3 ($P < 0.01$), and PANC-1 ($P < 0.01$) cells compared with HPDE6 cells (Fig. 2a). To investigate the functional effects of high expression of IRAIN in PC cells, we modulated its expression through transfection of IRAIN siRNA to knock down its expression. qPCR analysis of IRAIN levels was performed 48 h post-transfection. Results showed that IRAIN expression was significantly reduced by

si-IRAIN transfection when compared with control cells (Fig. 2b).

Table 2 Correlation between IRAIN expression and clinicopathological characteristics of patients with PC ($n = 37$)

Characteristics	N	IRAIN level		P values
		Low	High	
Total cases	37	18	19	
Gender				0.728
Male	24	10	14	
Female	13	6	7	
Age (years)				1.000
<60	18	9	9	
≥ 60	19	9	10	
Tumor size (cm)				0.049
<2	20	13	7	
≥ 2	17	5	12	
Differentiation				0.091
Well/moderate	13	9	4	
Poor	24	9	15	
TNM stage				0.020
I/II	15	11	4	
III/IV	22	7	15	
Lymph node metastasis				0.020
Negative	15	11	4	
Positive	22	7	15	

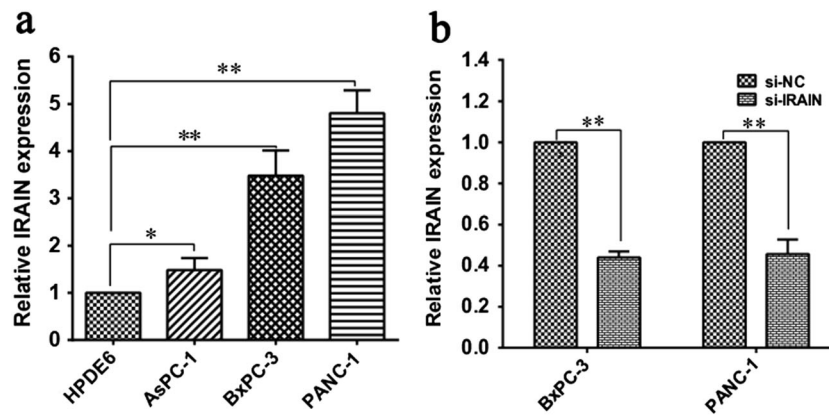


Fig. 2 Increased IRAIN expression in PC cells. **a** qPCR analysis of IRAIN expression in HPDE6 cells (immortalized human pancreatic ductal epithelial cells) and PC cells. **b** qPCR analysis of IRAIN

expression levels following treatment of BxPC-3 and PANC-1 cells with siRNAs against IRAIN. Bars: SD, * $P < 0.05$, ** $P < 0.01$, from three independent experiments

Knockdown of IRAIN induced PC cell apoptosis and cell cycle arrest

To further assess the role of IRAIN in PC cells, we performed an MTT assay. The results revealed that knockdown of IRAIN expression significantly inhibited cell viability both in BxPC-3 and PANC-1 cell lines compared with control cells (Fig. 3a, b). Similarly, the result of colony formation assays showed that clonogenic survival was strikingly decreased following

inhibition of IRAIN in both BxPC-3 and PANC-1 cell lines (Fig. 3c, d).

Next, we examined the effects of knockdown of IRAIN on apoptosis using flow cytometry. After transfection with si-IRAIN or si-NC for 48 h, results showed that the percentage of apoptotic cells was significantly increased in the treated group compared to the control (Fig. 4a, b). Consistent with this finding, the results of TUNEL staining assay in PC cells also showed that the

Fig. 3 Effect of IRAIN on PC cell viability in vitro. **a, b** MTT assays were used to determine the cell viability of BxPC-3 and PANC-1 cells transfected with siRNAs against IRAIN. **c, d** Colony-forming assays were conducted to determine the proliferation of BxPC-3 and PANC-1 cells transfected with siRNAs against IRAIN. Bars: SD, * $P < 0.05$, ** $P < 0.01$, from three independent experiments

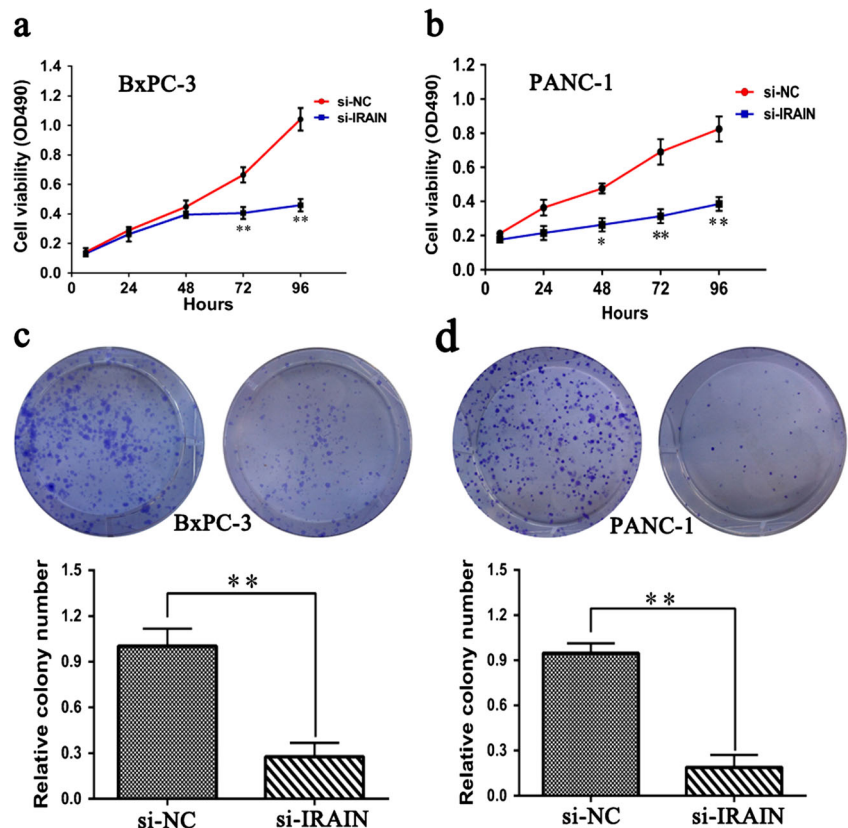
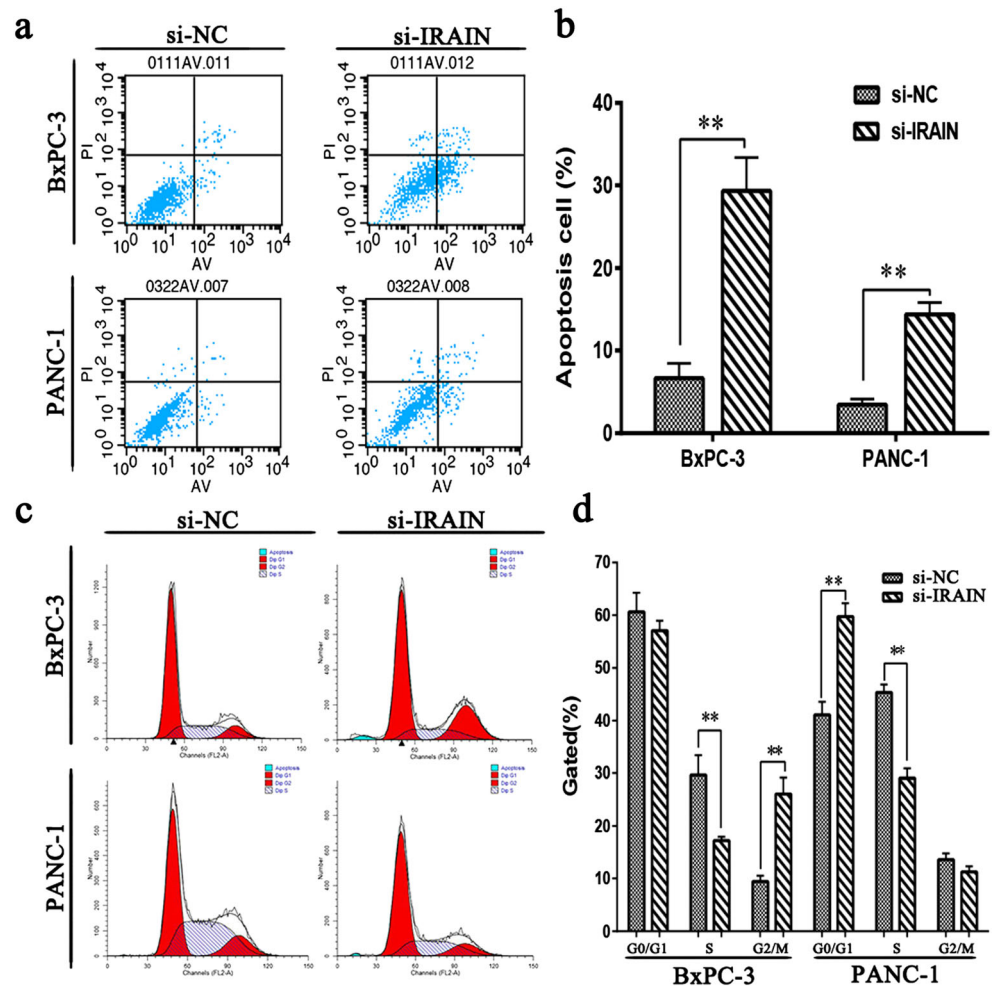


Fig. 4 Knockdown of IRAIN-induced PC cell apoptosis. **a, b** Knockdown of IRAIN-induced apoptosis in BxPC-3 and PANC-1 cells. **c, d** Cell cycle analyses of BxPC-3 and PANC-1 cells. **Bars:** SD, * $P < 0.05$, ** $P < 0.01$, from three independent experiments



knockdown of IRAIN resulted in a higher number of apoptotic cells compared with the controls in both BxPC-3 and PANC-1 cell lines (Fig. 5a). Subsequently, to determine whether the role of IRAIN in the proliferation of PC cells was mediated by inhibition of cell cycle progression, we performed flow cytometry analysis. The results showed that knockdown of IRAIN led to a significant accumulation of cells in the G2/M-phase ($P < 0.05$), while it decreased the proportion of cells in the S phase compared to the control in BxPC-3 cell lines (Fig. 4c, d). Interestingly, the knockdown of IRAIN drove progression beyond the G1/G0 transition in PANC-1 cell lines—and the percentage of cells in the G1/G0 phase in PANC-1/si-IRAIN was significantly higher than that of PANC-1/si-NC cells (Fig. 4c, d). In addition, some apoptosis and cell cycle-related protein levels were detected, and the results showed that the levels of cleaved caspase-3 and P21 were decreased after IRAIN knockdown, and Bcl-2 level was significantly increased (Fig. 5b). These data demonstrate that knockdown of IRAIN could induce PC cell apoptosis and cell cycle arrest.

IRAIN suppressed KLF2 and P15 transcription by interacting with LSD1 and EZH2

As PC cell apoptosis and cell cycle arrest after IRAIN knockdown were observed, we further explored its underlying molecular mechanisms using BxPC-3 as a cell model. To identify the downstream targets of IRAIN, we investigated potential target genes involved in the cell cycle via qPCR (Supplementary Fig. S1a). Among these analyzed genes, we found that KLF2 and P15 (CDKN2B) were two of the most significantly upregulated genes after IRAIN knockdown (Fig. 6a). Meanwhile, the western blot assays showed the same results (Fig. 6b, c), which indicated that KLF2 and P15 could be IRAIN novel targets in PC cells. Since KLF2 and P15 are two key tumor suppressors responsible for cell apoptosis and cell cycle control [16–18], we hypothesized that IRAIN may contribute to PC cell apoptosis and cell cycle arrest through negatively regulating the expression of KLF2 and p15.

Previous studies have shown that many lncRNAs perform their biologic function through interaction with one

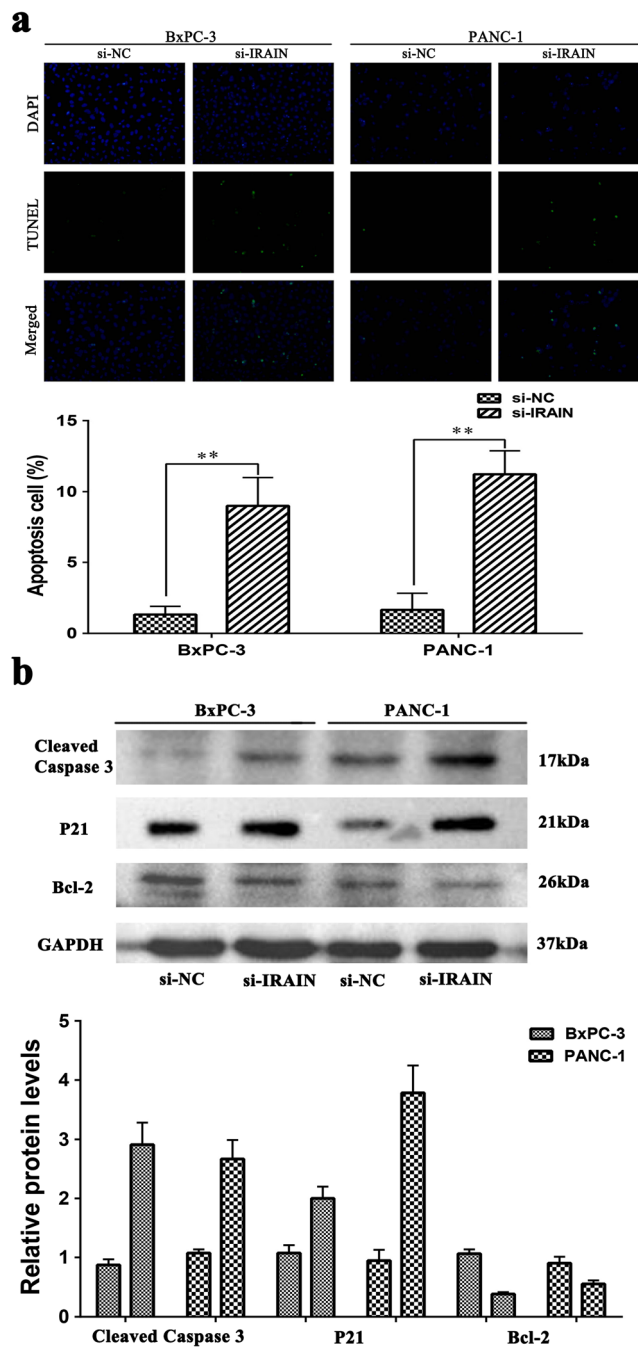


Fig. 5 Effect of IRAIN on PC cell apoptosis confirmed by TUNEL assay and western blot analysis. **a** TUNEL staining assays were performed to analyze cell apoptosis after IRAIN knockdown. The images of TUNEL-positive cells were captured by a fluorescence microscope ($\times 200$). Quantitative result of TUNEL assay was analyzed. **b** Effect of knockdown of IRAIN on cell cycle- and apoptosis-related protein expression. Representative images and data based on three independent experiments. Bars: SD, $*P < 0.05$, $**P < 0.01$

or more RBPs [19, 20]. Therefore, we conducted RIP analysis to examine IRAIN's binding with LSD1 and EZH2. As shown in Fig. 6d, endogenous IRAIN was enriched in the anti-LSD1 and anti-EZH2 RIP fractions

in BxPC-3 cells. Furthermore, our qPCR results also showed that inhibition of LSD1 expression led to increased KLF2 and P15 expression, while knockdown of EZH2 only upregulated KLF2 expression (Fig. 6e, f). Furthermore, we examined whether IRAIN regulated KLF2 and P15 in pancreatic cancer patients. qPCR assay was performed to evaluate the expression levels of KLF2, P15, and IRAIN in 37 paired PC and adjacent non-tumor pancreas tissues. As shown in Fig. 6g, h, KLF2 and P15 mRNA levels negatively correlated with the expression of IRAIN.

These results indicate that IRAIN can directly bind to EZH2 and LSD1 complexes and repress KLF2 and P15 in pancreatic cancer.

Discussion

While the dysregulation and biological function of lncRNAs are associated with many types of cancer, their underlying mechanisms or disease-causing events are not fully understood [21]. Recently, several lncRNAs, including HOXA transcript at the distal tip (HOTTIP) [22], HOX transcript antisense RNA (HOTAIR) [23], and metastasis-associated lung adenocarcinoma transcript 1 (MALAT-1) [24], were confirmed to play an important role in the progression of pancreatic cancer.

Moreover, based on the findings of several studies, lncRNAs are becoming potential prognostic biomarkers in pancreatic cancer patients [25]. For example, Ye et al. have found that lncRNA AFAP1-AS1 is upregulated in pancreatic cancer tissues and serves as a negative prognostic factor for lymph node metastasis, perineural invasion, and poor survival in pancreatic cancer patients [26]. Therefore, understanding the roles of lncRNAs as tumor suppressors or oncogenes will help to identify novel potential biomarkers for early diagnosis, accurate prognosis prediction, and new epigenetic molecular targets for treating pancreatic cancer patients.

Our previous study showed that IRAIN was significantly increased in human non-small cell lung cancer (NSCLC) tissues and showed a significant correlation with tumor size and smoking status. Moreover, silencing of IRAIN could suppress cell growth of NSCLC cells by blocking cells in the G1/S phase [15]. However, the clinical significance and potential role of IRAIN in PC remain unclear. In this study, we found that IRAIN is significantly increased and is correlated with larger tumor sizes, advanced TNM stages, and lymph node metastasis in PC patients. Further experiments revealed that knockdown of IRAIN induced cell apoptosis and inhibited cell proliferation in both BxPC-3 and PANC-1 cells. Interestingly, molecular mechanistic investigation showed

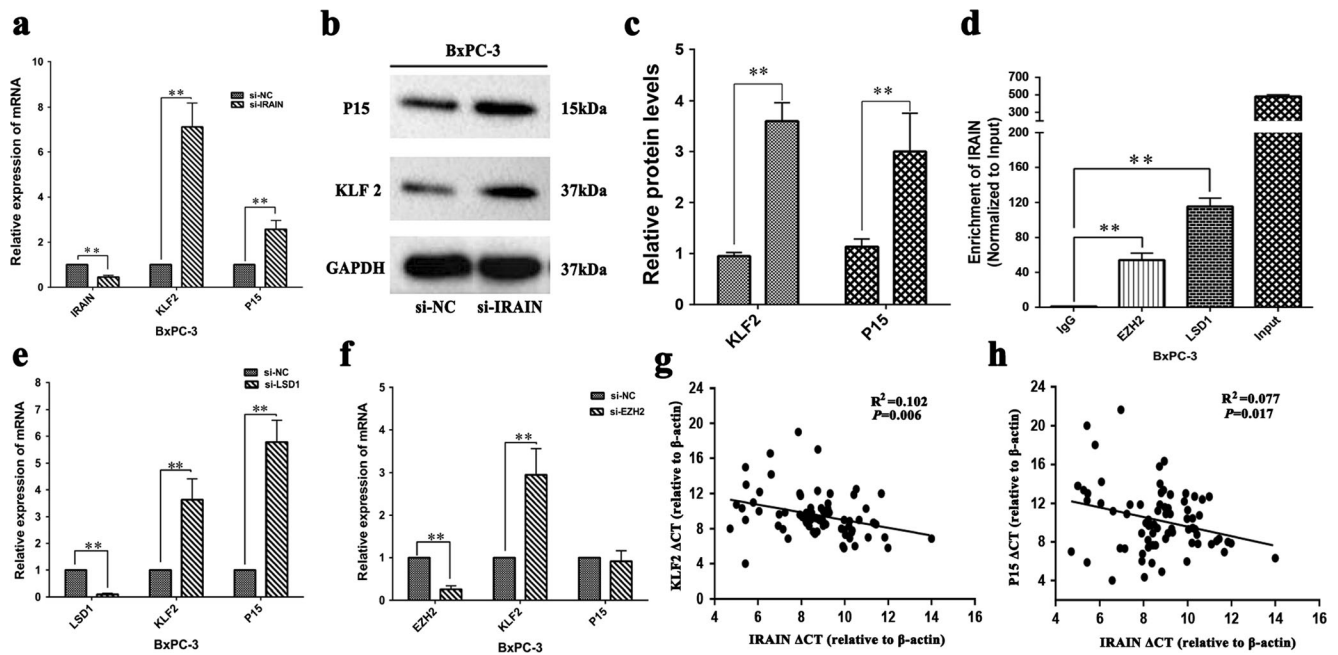


Fig. 6 IRAIN interacted with LSD1 and EZH2 and suppressed KLF2 and P15 expression. **a** KLF2 and P15 mRNA levels were determined by qPCR upon IRAIN knockdown. **b, c** The KLF2 and P15 protein levels were determined by western blot in IRAIN knockdown BxPC-3 cells. **d** RNA levels in immunoprecipitates were determined by qPCR. Expression levels of IRAIN RNA were presented as fold enrichment

relative to IgG immunoprecipitates. **e, f** KLF2 and P15 expression levels were determined by qPCR when EZH2 or LSD1 was knocked down in BxPC-3 cells. **g, h** KLF2 and P15 expression levels were negatively correlated IRAIN expression level in our expression cohort via qPCR. Bars: SD, * $P < 0.05$, ** $P < 0.01$, from three independent experiments

that knockdown of IRAIN led to a significant accumulation of BxPC-3 cells in the G2/M phase, while significantly stalling PANC-1 cells at the G0/G1 phase, compared with cells transfected with si-NC. The inconsistency of IRAIN in regulating the cell cycle in BxPC-3 and PANC-1 cell lines may be due to its differential expression phenotype. Similar results have been previously observed by Zhang [27]. Furthermore, we demonstrated that IRAIN was associated with two key RBPs, LSD1 and EZH2. This association was also required for epigenetic repression of downstream targets, including KLF2 and P15, thus contributing to the regulation of PC cell apoptosis and proliferation. These findings will help to better understand the role of IRAIN in inducing cell apoptosis and cell cycle arrest.

It has been confirmed that most lncRNAs perform their biological function by binding to RBPs [19, 28]. The histone demethylase LSD1 plays an important role in the epigenetic regulation of gene transcription. A previous study demonstrated that LSD1 expression was increased in PC tissues, and elevated LSD1 expression was associated with poor prognosis of PC patients [29]. Khail et al. [12] reported that approximately 20 % of the lncRNAs expressed in various cell types are bound to polycomb repressive complex 2 (PRC2). EZH2 is an essential component of the PRC2 complex, which is

overexpressed in multiple cancers [30]. Recent studies have found that EZH2 is recruited by lncRNA MALAT-1 and that subsequent involvement of the complex in the repression of E-cadherin promotes pancreatic cancer migration and invasion [31]. Our experiments demonstrated that IRAIN can directly interact with EZH2 and LSD1 complexes and repress KLF2 and P15 in pancreatic cancer. The functional role of KLF2 and P15 has been previously illustrated in pancreatic cancer [32, 33]. Numerous findings have revealed that KLF2 and P15 can function as tumor suppressors [18, 34]. Our results also showed that IRAIN was inversely correlated with KLF2 and P15 expression in pancreatic cancer tissues. These data indicated that IRAIN may play a critical role in EZH2- and LSD1-mediated repression of tumor suppressors in PC cells. In addition, further analyses are needed to better understand the mechanisms between EZH2/LSD1 and KLF2/P15.

In conclusion, we revealed that lncRNA IRAIN plays a key role in the progression of PC by regulating the expression of KLF2 and P15 via LSD1 and EZH2. Our findings indicate that IRAIN may be a potential therapeutic target in PC. However, since other possible downstream targets and mechanisms that underline regulatory behaviors were not investigated in our study, they remain to be further investigated.

Acknowledgments This work was supported by the Six Talents Peak Project of Jiangsu Province (WSN-050), the Key Project supported by Medical Science and Technology Development Foundation, Nanjing Department of Health (YKK13178), and the Medical Science and Technology Development Foundation, Nanjing Medical University (2014NJMUZD074).

Compliance with ethical standards Informed consent was obtained from all patients. Our study was approved by the Research Ethics Committee of Nanjing Medical University, China.

Conflicts of interest None

References

- Siegel RL, Miller KD, Jemal A. Cancer statistics, 2015. *CA Cancer J Clin.* 2015;65(1):5–29.
- Hussain SP. Pancreatic cancer: current progress and future challenges. *Int J Biol Sci.* 2016;12(3):270–2.
- Wolfgang CL et al. Recent progress in pancreatic cancer. *CA Cancer J Clin.* 2013;63(5):318–48.
- Ponting CP, Oliver PL, Reik W. Evolution and functions of long noncoding RNAs. *Cell.* 2009;136(4):629–41.
- Guttman M et al. Chromatin signature reveals over a thousand highly conserved large non-coding RNAs in mammals. *Nature.* 2009;458(7235):223–7.
- Prensner JR, Chinnaiyan AM. The emergence of lncRNAs in cancer biology. *Cancer Discov.* 2011;1(5):391–407.
- Lian, Y., et al., The long noncoding RNA HOXA transcript at the distal tip promotes colorectal cancer growth partially via silencing of p21 expression. *Tumour Biol*, 2015.
- Li Y et al. HBXIP and LSD1 Scaffolded by lncRNA Hotair mediate transcriptional activation by c-Myc. *Cancer Res.* 2016;76(2):293–304.
- Nie FQ et al. Long noncoding RNA ANRIL promotes non-small cell lung cancer cell proliferation and inhibits apoptosis by silencing KLF2 and P21 expression. *Mol Cancer Ther.* 2015;14(1):268–77.
- Zhang H et al. PLK1 and HOTAIR accelerate proteasomal degradation of SUZ12 and ZNF198 during hepatitis B virus-induced liver carcinogenesis. *Cancer Res.* 2015;75(11):2363–74.
- Tsai MC et al. Long noncoding RNA as modular scaffold of histone modification complexes. *Science.* 2010;329(5992):689–93.
- Khalil AM et al. Many human large intergenic noncoding RNAs associate with chromatin-modifying complexes and affect gene expression. *Proc Natl Acad Sci U S A.* 2009;106(28):11667–72.
- Zhou, Q., et al., Long noncoding RNA PVT1 modulates thyroid cancer cell proliferation by recruiting EZH2 and regulating thyroid-stimulating hormone receptor (TSHR). *Tumour Biol*, 2015.
- Zang, C., et al., Long non-coding RNA LINC01133 represses KLF2, P21 and E-cadherin transcription through binding with EZH2, LSD1 in non small cell lung cancer. *Oncotarget*, 2016.
- Feng J et al. A novel long noncoding RNA IRAIN regulates cell proliferation in non small cell lung cancer. *Int J Clin Exp Pathol.* 2015;8(10):12268–75.
- Zhang W et al. Kruppel-like factor 2 suppresses mammary carcinoma growth by regulating retinoic acid signaling. *Oncotarget.* 2015;6(34):35830–42.
- Xu TP et al. SP1-induced upregulation of the long noncoding RNA TINCR regulates cell proliferation and apoptosis by affecting KLF2 mRNA stability in gastric cancer. *Oncogene.* 2015;34(45):5648–61.
- Wolff L, Bies J. p15Ink4b functions in determining hematopoietic cell fates: implications for its role as a tumor suppressor. *Blood Cells Mol Dis.* 2013;50(4):227–31.
- Ferre F, Colantoni A, Helmer-Citterich M. Revealing protein-lncRNA interaction. *Brief Bioinform.* 2016;17(1):106–16.
- Mohamadkhani A, Long Noncoding RNA. In interaction with RNA binding proteins in hepatocellular carcinoma. *Hepat Mon.* 2014;14(5):e18794.
- Tsai MC, Spitale RC, Chang HY. Long intergenic noncoding RNAs: new links in cancer progression. *Cancer Res.* 2011;71(1):3–7.
- Cheng Y et al. The long non-coding RNA HOTTIP enhances pancreatic cancer cell proliferation, survival and migration. *Oncotarget.* 2015;6(13):10840–52.
- Kim K et al. HOTAIR is a negative prognostic factor and exhibits pro-oncogenic activity in pancreatic cancer. *Oncogene.* 2013;32(13):1616–25.
- Jiao F et al. Long noncoding RNA MALAT-1 enhances stem cell-like phenotypes in pancreatic cancer cells. *Int J Mol Sci.* 2015;16(4):6677–93.
- Jin K et al. Noncoding RNAs as potential biomarkers to predict the outcome in pancreatic cancer. *Drug Des Devel Ther.* 2015;9:1247–55.
- Ye Y et al. High expression of AFAP1-AS1 is associated with poor survival and short-term recurrence in pancreatic ductal adenocarcinoma. *J Transl Med.* 2015;13:137.
- Zhang, Z.Y., et al., Loss of TINCR expression promotes proliferation, metastasis through activating EpCAM cleavage in colorectal cancer. *Oncotarget*, 2016.
- Li JH et al. Discovery of protein-lncRNA interactions by integrating large-scale CLIP-Seq and RNA-Seq datasets. *Front Bioeng Biotechnol.* 2014;2:88.
- Qin Y et al. LSD1 sustains pancreatic cancer growth via maintaining HIF1 α -dependent glycolytic process. *Cancer Lett.* 2014;347(2):225–32.
- Volkkel P et al. Diverse involvement of EZH2 in cancer epigenetics. *Am J Transl Res.* 2015;7(2):175–93.
- Han, T., et al., EZH2 promotes cell migration and invasion but not alters cell proliferation by suppressing E-cadherin, partly through association with MALAT-1 in pancreatic cancer. *Oncotarget*, 2016.
- Zhang, D., et al., KLF2 is downregulated in pancreatic ductal adenocarcinoma and inhibits the growth and migration of cancer cells. *Tumour Biol*, 2015.
- Li G et al. Reduced levels of p15INK4b, p16INK4a, p21cip1 and p27kip1 in pancreatic carcinoma. *Mol Med Rep.* 2012;5(4):1106–10.
- Kaczynski J, Cook T, Urrutia R. Sp1- and Kruppel-like transcription factors. *Genome Biol.* 2003;4(2).